Article

Discovery Medicine 2024; 36(191): 2386–2398
https://doi.org/10.24976/Discov.Med.202436191.220

A New Perspective for Improving COPD: Ginsenoside Rg3 Links SIRT1 to Inhibit Mitochondrial Autophagy

Yuanyuan Wang[1], Nianzhi Zhang[1,*], Feng Liu[2], Jing Zhou[1], Gang Teng[1], He Huang[1]

[1]Department of Respiratory Medicine, The First Affiliated Hospital of Anhui University of Chinese Medicine, 230031 Hefei, Anhui, China
[2]Second Internal Medicine, Mingguang City Hospital of Traditional Chinese Medicine, 239000 Chuzhou, Anhui, China
*Correspondence: dczhangnz@126.com (Nianzhi Zhang)
Published: 20 December 2024

Background: Chronic obstructive pulmonary disease (COPD) is a prevalent yet manageable respiratory condition. However, treatments presently used normally have side effects and cannot cure COPD, making it urgent to explore effective medications. The ginsenoside Rg3 (Rg3) has been shown to have anti-inflammatory and anti-tumor properties and can improve COPD. The primary objectives of this investigation were to explore the impact of Rg3 on COPD and delve into the associated mechanisms.
Methods: *In vitro* models exposed human bronchial epithelial cells (BEAS-2B) to cigarette smoke extract (CSE), and *in vivo* models induced COPD in mice through chronic inhalation of cigarette smoke (CS). Sirtuin 1 (SIRT1) expression was regulated via cell transfection or mice infection with recombinant lentiviruses. *SIRT1* mRNA levels were quantified using quantitative real-time reverse transcription polymerase chain reaction (qRT-PCR), and SIRT protein levels were assessed by western blot or enzyme-linked immunosorbent assays (ELISA). Mitophagy was evaluated by light chain 3 (LC3) II/I and phosphatase and tensin homolog (PTEN)-induced kinase 1 (PINK1) levels, and apoptosis was determined using terminal deoxynucleotidyl transferase dUTP nick-end labeling (TUNEL). Lung function was measured with the Buxco system, and inflammation was assessed via interleukin 6 (IL-6) and keratinocyte-derived cytokine (KC) levels in bronchial alveolar lavage fluid. Lung morphological impairments were determined through Hematoxylin and Eosin (H&E) staining and mean linear intercept (MLI) measurement.
Results: In BEAS-2B cells, CSE treatment caused a decrease in SIRT1 expression ($p < 0.01$) and an increase in LC3 II/I ($p < 0.01$) and PINK1 ($p < 0.01$), which were all reversed by Rg3 ($p < 0.01$), with 20 μM Rg3 performing the best and being used subsequently. CSE increased apoptosis of BEAS-2B cells ($p < 0.01$), which was reversed by Rg3 ($p < 0.01$). Upregulated SIRT1 further decreased levels of LC3 II/I ($p < 0.001$), PINK1 ($p < 0.001$), and cell apoptosis ($p < 0.001$) for CSE- and Rg3-treated cells, whereas downregulated SIRT1 reversely increased levels of LC3 II/I ($p < 0.001$), PINK1 ($p < 0.001$), and cell apoptosis ($p < 0.001$). The establishment of COPD caused a decrease in SIRT1 mRNA ($p < 0.001$), SIRT1 protein ($p < 0.001$), and lung functions ($p < 0.001$) whereas IL-6 ($p < 0.001$), KC ($p < 0.001$), lung impairment, and MLI ($p < 0.001$) were increased; all of these effects were reversed by Rg3 ($p < 0.001$). Moreover, the Rg3-induced reversion was furthered by SIRT1 upregulation ($p < 0.001$) and was disrupted by SIRT1 downregulation ($p < 0.001$).
Conclusion: Rg3, through activation of SIRT1, suppresses mitophagy and apoptosis, ameliorates COPD, and improves lung functions.

Keywords: ginsenoside Rg3; chronic obstructive pulmonary disease; SIRT1; mitochondrial autophagy; apoptosis

Introduction

Chronic obstructive pulmonary disease (COPD) is a prevalent, avoidable, and manageable chronic respiratory condition marked by persistent airflow limitation in the airways, leading to symptoms such as dyspnea, cough, and mucus production [1]. The most common cause of COPD is cigarette smoke exposure [2]. Through appropriate intervention, most COPD patients can better control symptoms and improve their quality of life. However, the existing COPD treatment drugs, mainly composed of a combination of bronchodilators and long-acting inhaled hormones, all have side effects during use [3,4]. And there is currently no treatment that can cure COPD. Hence, it is crucial to investigate novel pharmaceutical options for managing symptoms associated with COPD.

Ginsenoside Rg3 (Rg3) is a compound derived from red ginseng, with anti-inflammatory, anti-tumor, and other pharmacological properties [5,6]. It has been shown that Rg3 can treat and relieve symptoms of COPD by inhibiting neutrophil migration [7]. Sirtuins (SIRTs) are a family of deacetylases dependent upon NAD+ [8,9]. Studies have reported that sirtuin 1 (SIRT1) can regulate mitochondrial biogenesis [10,11], apoptosis [12,13], and autophagy [14,15] through the deacetylation of transcription factors and histones [16,17]. Because SIRT1 requires NAD+ cofactors to increase enzyme activity, it responds to changes in the environment, oxidative stress, and metabolism [18,19]. It

has been shown that SIRT1 can be covalently oxidized by cigarette smoke (CS)-derived oxidants/aldehydes, resulting in post-translational modification, inactivation, and protein degradation [20,21]. Relevant research results show that SIRT1 is reduced in the lungs of smokers and COPD patients [22]. Moreover, sodium hydrosulfide can up-regulate the expression of SIRT1 *in vivo* and *in vitro*, and protect lung bronchial epithelial cells from cigarette smoke extract (CSE)-induced epithelial-mesenchymal transition (EMT) [23]. Thus, activation of SIRT1 can help prevent and treat CS-induced airway remodeling.

Previous studies have proved that Rg3 can activate SIRT1 expression to reduce the inflammatory response of a rat myocardial infarction model [24], and can also reduce chondrocyte damage [25]. As a widely studied gene locus in mammals, SIRT1 can regulate a variety of cellular targets and functions and has corresponding therapeutic potential. However, the effects and mechanisms of Rg3 in the treatment of COPD are still unclear. We hypothesized that Rg3, as a SIRT1 activator, could suppress mitophagy and cell apoptosis in COPD, thus slowing the progression of COPD. Mitochondrial autophagy is a selective macroautophagy/autophagy that degrades dysfunctional or excessive mitochondria [26]. Mitochondrial damage induced by CS exposure accumulates in the process of COPD [27] and autophagy can eliminate damaged mitochondria. At the same time, studies have also shown that regulating apoptosis can improve COPD [28,29].

Therefore, in order to verify our hypothesis, we examined the effects of Rg3 on mitophagy and apoptosis in CS-induced COPD models *in vivo* and *in vitro*. The effect of Rg3 on COPD was evaluated by measuring the lung function of experimental animals. In addition, the potential involvement of the SIRT1 signaling pathway was analyzed.

Materials and Methods

Cell Culture

Human bronchial epithelial cells (BEAS-2B) (iCell-h023) were purchased from iCell Bioscience Inc. (Shanghai, China). The cells were cultured in Dulbecco's modified eagle medium (DMEM; iCell-0001, iCell Bioscience Inc., Shanghai, China) containing 10% fetal bovine serum (FBS; iCell-0500, iCell Bioscience Inc., Shanghai, China) and 1% penicillin-streptomycin (iCell-15140-122, iCell Bioscience Inc., Shanghai, China). The culturing condition was 37 °C, 70%–80% relative humidity, and 5% CO_2. Cells passed to the third generation were used for subsequent experiments. Cells have been verified by short tandem repeat (STR), and mycoplasma testing was performed before cells were used in order to avoid cell contamination.

Preparation of CSE

The preparation of CSE used *in vitro* was based on a previous study [30]. Briefly, 10 mL of serum-free sterile DMEM was added into a 60-mL plastic syringe and one puff of cigarette smoke (40 mL; 3R4F; University of Kentucky, Lexington, KY, USA) was drawn into this syringe and mixed with the medium for 30 seconds. During the mixing, the syringe was gently shaken. A total of 10 puffs were taken from one cigarette and for each puff, the procedure of mixing with DMEM was repeated. Consequently, one cigarette was used for 10 mL of aqueous CSE solution which was filtered by an aseptic 0.22-μm filter to exclude bacteria and particles to acquire the 100% CSE solution. The procedure for preparing CSE used *in vivo* was similar to that for CSE used *in vitro* except that the 10 mL DMEM was substituted with 2 mL sterile phosphate-buffered saline (PBS; C0551A, Beyotime, Shanghai, China).

Cell Treatments

The design of cell treatments was based on the previous study with some modifications [7]. The acquired 100% CSE solution was diluted in serum-free DMED and was standardized to 10% CSE which was used for culturing BEAS-2B cells which act as the *in vitro* CS exposure model. Rg3 was purchased (SML0184, Sigma-Aldrich, Saint Louis, MO, USA) and added into culture medium at certain concentrations for culturing cells. The groups of cells with different treatments are listed in Table 1.

Transfection

The lentiviruses containing pCMV2-GV146-GFP vector inserted by the short hairpin (sh)RNA of human *SIRT1* (sh-*SIRT1*; 5′-CACCGCCTCACATGCAAGCTCTAGTCGAAACTAGAGCTTGCATGTGAGGC-3′) for cell transfection or shRNA of mice *Sirt1* (sh-*Sirt1*; 5′-CACCGCACCGATCCTCGAACAATTCCGAAGAATTGTTCGAGGATCGGTGC-3′) for mice transfection or the negative control shRNA (sh-NC; 5′-ACCGGCCTAAGGTTAAGTCGCCCTCGCTGAGCGAGGGCGACTTAACCTTAGGTTTTTGAATTC-3′) for cell transfection or the negative control (sh-nc; 5′-AAAAGCTACACTATCGAGCAATTTTGGATCCAAAATTGCTCGATAGTGTAGC-3′) for mice transfection were obtained for downregulating *SIRT1* expression in BEAS-2B cells. The lentiviruses containing blank pCMV2-GV146-GFP vector (OE-NC/OE-nc), the pCMV2-GV146-GFP-*SIRT1* expression plasmid for cell transfection (OE-*SIRT1*; inserted by full-length of human *SIRT1*, NC_000010), and pCMV2-GV146-GFP-*Sirt1* expression plasmid for mice transfection (OE-*Sirt1*; inserted by full-length of mice Sirt1, NC_000076) were obtained for upregulating *SIRT1* expression in BEAS-2B cells and *Sirt1* expression in mice. All lentiviruses were constructed by GeneChem (Shanghai, China). The transfections of CSE-treated cells were performed using the Lipofectamine™ 3000 transfection reagent (L3000150, Invitrogen, Carlsbad, CA, USA) according to the manufacturer's instructions.

Table 1. Cell grouping and administration.

Group (n = 5)	Methods of intervention
Control	BEAS-2B cells cultured normally
CSE	BEAS-2B cells were treated with 10% CSE for 12 hours and then cultured normally
CSE+High	BEAS-2B cells were treated with 10% CSE for 12 hours and then treated with 40 μM Rg3
CSE+Medium	BEAS-2B cells were treated with 10% CSE for 12 hours and then treated with 20 μM Rg3
CSE+Low	BEAS-2B cells were treated with 10% CSE for 12 hours and then treated with 10 μM Rg3

CSE, cigarette smoke extract; Rg3, ginsenoside Rg3; BEAS-2B, bronchial epithelial cells.

Mice Preparation

This study has been approved by the ethics committee of Anhui University of Chinese Medicine (approval no. AHUCM-rats-2021064). Thirty-five female BALB/C mice (8 weeks old), weighing 30 ± 2 g, were procured from Beijing Vital River Laboratory Animal Technology Co., Ltd. (lot number: 211, Beijing, China). The mice were provided with standard food and water and housed under conditions of 21–23 °C, 40%–60% relative humidity, and a 12-hour light/dark cycle.

Grouping and Treatments of Mice Models

Treatments for mice were according to the previous study with some modifications [7]. For mediating Sirt1 expression in mice, lentiviruses used for cell transfection were diluted into PBS (C0551A, Beyotime, Shanghai, China) to achieve a concentration of 10^8 CFU/mL and the mixture was administered to the mice by nasal drip (30 μL). To expose the mice to CS, they were initially immobilized using restraint, and a snug latex-sealed nose cap was securely placed over the nose and mouth, extending beyond the whiskers. Subsequently, the restrained mice were positioned in an inhalation tower designed to maintain the required atmospheric conditions. Cigarette smoke (3R4F, University of Kentucky, Lexington, KY, USA) with a total suspended particle concentration of 400 mg/m^3 was delivered to the mice through the tower. Mice in the Control group were exposed to room air and the remaining 30 mice in other groups were exposed to CS for 2 times/day and 1 h/time. The CS exposure was performed for 14 weeks. The administration of lentiviruses and Rg3 began in the 12th week and was performed daily. After nasal drip of lentiviruses, the Rg3 (40 mg/kg) was administrated intragastrically at least 2 hours before CS inhalation. The final treatment was completed at the end of the 14th week; 24 hours after the last treatment, the mice were euthanized via intraperitoneal injection of sodium pentobarbital (110 mg/kg) for subsequent experiments. After the mice were euthanized, a thoracoabdominal incision was made to expose the lungs. The lungs were perfused with physiological saline to clear blood. Using sterile instruments, specific portions of lung tissue were carefully excised or dissected. The grouping and treatments for experimental animals are shown in Table 2.

Lung Function Measurements and Sample Collection

Mice were fixed and a cannula used for invasive lung function testing was inserted into the trachea. The test was performed using the Buxco pulmonary function testing system (FinePointe; Data Sciences International, St. Paul, MN, USA). Afterwards, the bronchial alveolar lavage fluid (BALF) was collected by separating the trachea and attaching it to a syringe containing sterile PBS (1 mL) which was used for washing the pulmonary cavity 3 times. The retrieved fluid was collected as BALF. Ultimately, mouse lungs were retrieved, rinsed with PBS, fixed in 4% paraformaldehyde (P0099, Beyotime, Shanghai, China), and then embedded in paraffin.

Hematoxylin and Eosin (H&E) Staining

The lung tissues, embedded in paraffin, were sectioned into 4-μm slices and subjected to staining with Hematoxylin and Eosin (H&E; C0105S, Beyotime, Shanghai, China) as per the manufacturer's instructions. Microscopic observation of the histopathological features of the lung tissues was conducted using a microscope (CKX53, OLYMPUS, Tokyo, Japan). The mean linear intercept (MLI) was determined using ImageJ software (1.48, National Institutes of Health, Rockville, MD, USA), considering the number of intercepts, the length of a line, and the frequency of lines placed on the sections [31].

Quantitative Real-time Reverse Transcription Polymerase Chain Reaction (qRT-PCR)

Total RNA extraction was carried out using the TRIzol reagent (DP424, Tiangen, Beijing, China), followed by reverse transcription into cDNA using the FastQuant cDNA Synthesis Kit (KR116, Tiangen, Beijing, China). The qRT-PCR reaction mixture was composed using the SYBR Green One-Step qRT-PCR Kit (D7268S, Beyotime, Shanghai, China), and the reaction was conducted in a PCR instrument (LightCycler96, Roche, Shanghai, China). β-actin served as the internal reference, and the expression data for the target genes were analyzed using the $2^{-\Delta\Delta CT}$ method. The sequences of used primers were: human *SIRT1* (forward, 5′-TGCCGGAAACAATACCTCCA-3′; reverse 5′-AGACACCCCAGCTCCAGTTA-3′), human β-actin (forward, 5′-CCTCGCCTTTGCCGATCC-3′; reverse 5′- GGATCTTCATGAGGTAGTCAGTC-3′), mouse

Table 2. Grouping and treatments of mice models.

Group (n = 5)	Methods of intervention
NC	Mice were normally raised and with no treatments
Model	Mice were treated with CS exposure for 14 weeks and intragastrically administered normal saline (10 mL/kg) from the 12th week
Model+Rg3	Mice were treated with CS exposure for 14 weeks and intragastrically administered Rg3 (40 mg/kg) from the 12th week
Model+Rg3+OE-nc	Mice were treated with CS exposure for 14 weeks and from the 12th week, mice received a nasal drip of OE-nc solution (dissolved in PBS; 10^8 CFU/mL, 30 µL) and were intragastrically administered Rg3 (40 mg/kg)
Model+Rg3+OE-Sirt11	Mice were treated with CS exposure for 14 weeks and from the 12th week, mice received a nasal drip of OE-Sirt1 solution (dissolved in PBS; 10^8 CFU/mL, 30 µL) and were intragastrically administered Rg3 (40 mg/kg)
Model+Rg3+sh-nc	Mice were treated with CS exposure for 14 weeks and from the 12th week, mice received a nasal drip of sh-nc solution (dissolved in PBS; 10^8 CFU/mL, 30 µL) and were intragastrically administered Rg3 (40 mg/kg)
Model+Rg3+sh-Sirt1	Mice were treated with CS exposure for 14 weeks and from the 12th week, mice received a nasal drip of sh-Sirt1 solution (dissolved in PBS; 10^8 CFU/mL, 30 µL) and were intragastrically administered Rg3 (40 mg/kg)

CS, cigarette smoke; PBS, phosphate-buffered saline; Sirt1, sirtuin 1; OE-nc, lentiviruses containing blank vectors; OE-Sirt1, lentiviruses containing Sirt1 overexpression plasmid; sh-nc, lentiviruses containing vector inserted with negative control short hairpin (sh)RNA; sh-Sirt1, lentiviruses containing vector inserted with shRNA against Sirt1.

Sirt1 (forward, 5′-GACGCTGTGGCAGATTGTTA-3′; reverse 5′-GGAATCCCACAGGAGACAGA-3′) and mouse β-actin (forward, 5′-GTCGTACCACAGGCATTGTGATGG-3′; reverse 5′-GCAATGCCTGGGTACATGGTGG-3′).

Western Blot Assay

Total proteins were extracted using the Radio Immunoprecipitation Assay (RIPA) method (P0013, Beyotime, Shanghai, China), and the protein concentration was determined using the bicinchoninic acid (BCA) protein assay kit (P0012S, Beyotime, Shanghai, China). Separation of proteins was achieved using a 10% SDS-PAGE gel (P0012, Beyotime, Shanghai, China), followed by transfer to membranes (IPVH15150, Millipore Sigma, Billerica, MA, USA). The membranes were then incubated overnight at 4 °C with primary antibodies, including anti-SIRT1 (1:1000 dilution, ab110304, Abcam, Cambridge, MA, USA), anti-light chain 3 (LC3) (1:1000 dilution, ab192890, Abcam, Cambridge, MA, USA), anti-phosphatase and tensin homolog (PTEN)-induced kinase 1 (PINK1) (1:1000 dilution, ab216144, Abcam, Cambridge, MA, USA), and anti-glyceraldehyde-3-phosphate dehydrogenase (GAPDH) (1:1000 dilution, Cat. No. ab8245, Abcam, Cambridge, MA, USA). Subsequently, the membranes were incubated with the secondary antibody horseradish-peroxidase (HRP) goat anti-mouse IgG (1:1000 dilution, Cat. no. A0216, Beyotime, Shanghai, China) at room temperature for 2 hours. Protein visualization was achieved using the enhanced chemiluminescence kit (P0018S, Beyotime, Shanghai, China), and the analysis was conducted using ImageJ software (1.48, National Institutes of Health, Rockville, MD, USA).

Apoptosis Assay

The membrane-breaking solution (Pinofei Biological Technology Co., Ltd., Wuhan, China) was carefully applied to the cell slides or tissue sections, which were then subjected to digestion with protease K (39450-01-6, Roche, Basel, Switzerland). Following this, the slides were incubated overnight at 4 °C in the terminal deoxynucleotidyl transferase dUTP nick-end labeling (TUNEL) reagent (11684817910, Roche, Basel, Switzerland). After staining the nucleus with DAPI (C1002, Beyotime, Shanghai, China), the slides were sealed and observed using a microscope (CKX53, OLYMPUS, Tokyo, Japan).

Enzyme-linked Immunosorbent Assays (ELISA)

The BALF obtained was subjected to centrifugation at 3000 rpm and 4 °C for 10 minutes. The resulting supernatant was collected, and the levels of inflammatory cytokines were assessed using the mouse kits for SIRT1 (ab206983, Abcam, Cambridge, MA, USA), interleukin 6 (IL-6; ab222503, Abcam, Cambridge, MA, USA), and keratinocyte-derived cytokine (KC; EMCXCL1, Invitrogen, Carlsbad, CA, USA) following the provided instructions.

Statistical Analysis

GraphPad Prism 7.0 software (GraphPad Software Inc., San Diego, CA, USA) was employed for statistical analysis. Results were expressed as mean ± standard de-

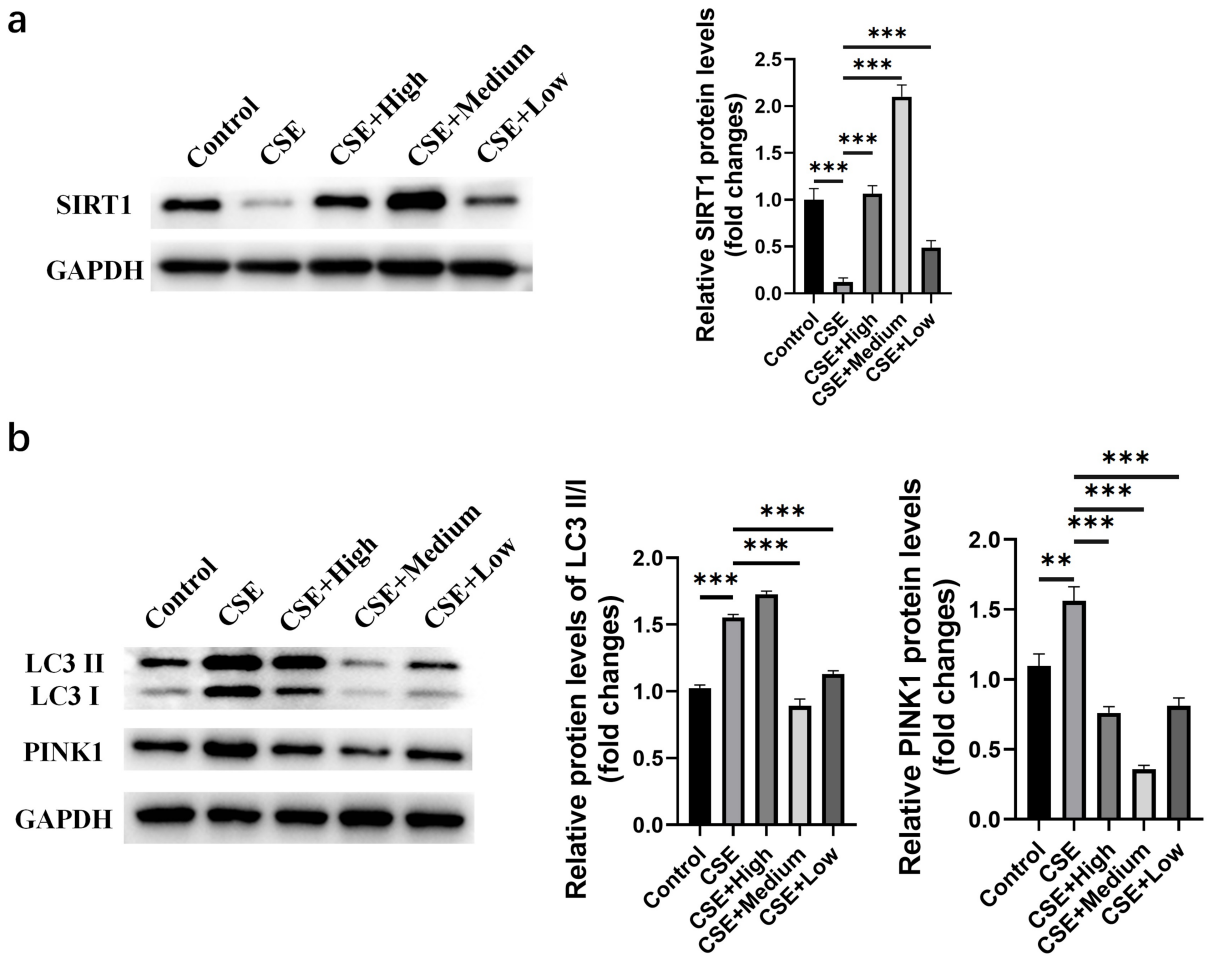

Fig. 1. Rg3 upregulated SIRT1 expression and inhibited mitophagy in cigarette smoke extract (CSE)-treated BEAS-2B cells. (a) The expression level of SIRT1 protein. (b) Western blot detection of mitophagy-related proteins. N = 5. Rg3, ginsenoside Rg3; Control, normally cultured BEAS-2B cells; CSE, BEAS-2B cells treated with cigarette smoke extract; CSE+High, BEAS-2B cells treated with CSE and 80-μM Rg3; CSE+Medium, BEAS-2B cells treated with CSE and 40-μM Rg3; CSE+Low, BEAS-2B cells treated with CSE and 20-μM Rg3; SIRT1, sirtuin 1; LC3, light chain 3; PINK1, phosphatase and tensin homolog (PTEN)-induced kinase 1; GAPDH, glyceraldehyde-3-phosphate dehydrogenase. $^{**}p < 0.01$, $^{***}p < 0.001$.

viation (SD). *T*-tests were used for comparisons between two groups, and one-way analysis of variance (ANOVA) was used for multiple groups, followed by Newman–Keuls post hoc tests. p values < 0.05 were considered statistically significant.

Results

Rg3 Upregulated SIRT1 Expression, and Downregulated Mitophagy and Apoptosis in CSE-treated BEAS-2B Cells

As shown in Fig. 1a, the protein expression level of SIRT1 in the CSE group was lower than that in the Control group ($p < 0.001$). However, the expression level of SIRT1 was reversely upregulated after using Rg3 at the high ($p < 0.001$), medium ($p < 0.001$), and low ($p < 0.001$) concentrations, and the medium concentration of Rg3 (40 μM) possessed the strongest capacity for upregulation of SIRT1. Changes in mitophagy-related proteins are shown in Fig. 1b. The levels of LC3 II/I and PINK1 protein in BEAS-2B cells were higher in the CSE group compared with the Control group (LC3 II/I, $p < 0.001$; PINK1, $p < 0.01$). The increase in LC3 II/I was reversed by the addition of 40 μM Rg3 ($p < 0.001$) and 80 μM Rg3 ($p < 0.001$). Similarly, the increase in PINK1 was reversed by the addition of 20 μM Rg3 in ($p < 0.001$), 40 μM Rg 3 ($p < 0.001$) and 80 μM Rg3 ($p < 0.001$). Together, these results demonstrated that Rg3 could activate SIRT1 and suppress mitophagy in CSE-treated BEAS-2B cells. According to the results in Fig. 1, Rg3 with a medium level of concentration (40 μM) had the strongest effect on activation of SIRT1 and decreasing mitophagy-related proteins; therefore, we used 40-μM Rg3 for the subsequent experiment. As shown in Fig. 2, the apoptosis rate of cells in the CSE group was

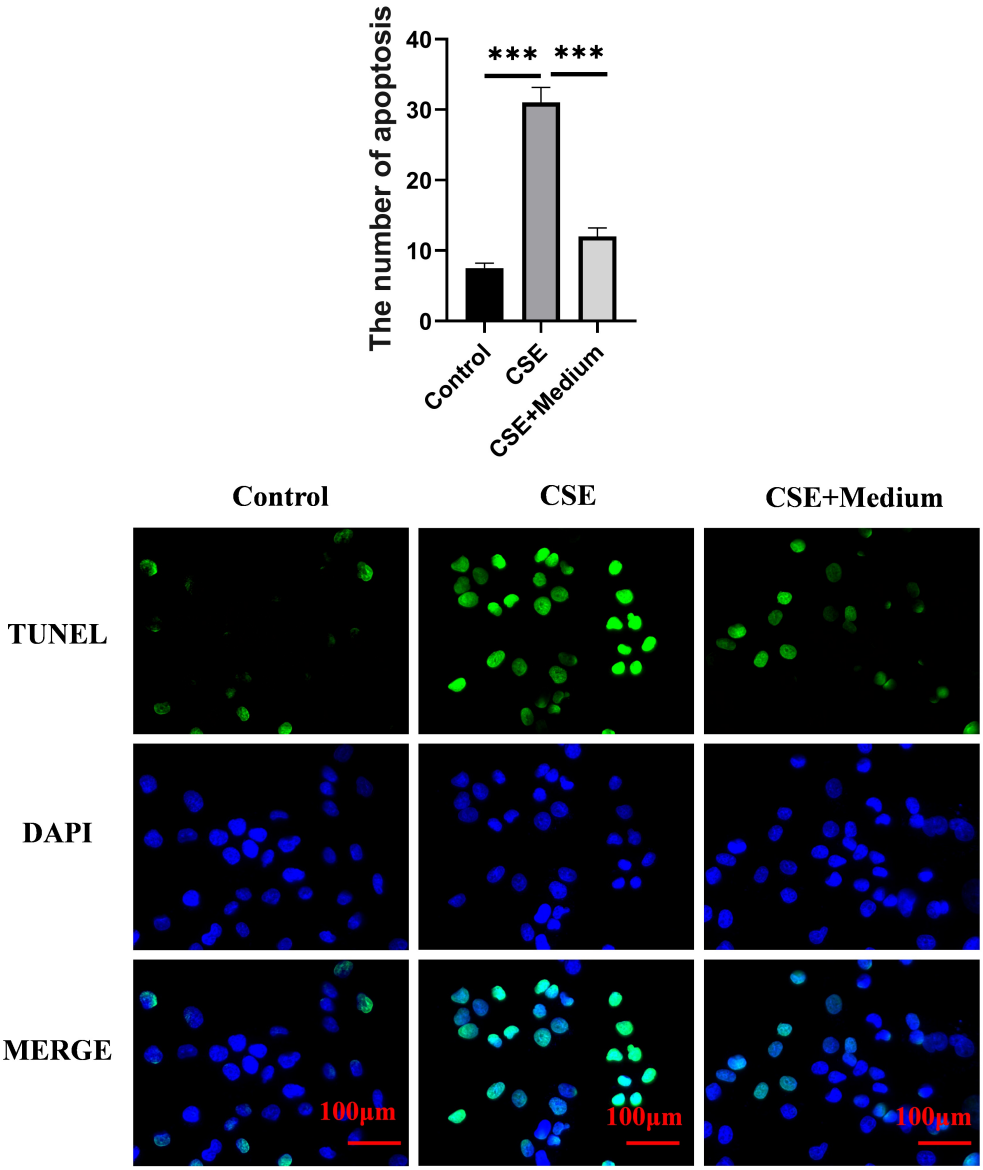

Fig. 2. Ginsenoside Rg3 suppressed apoptosis of CSE-treated BEAS-2B cells. Apoptosis was detected by the TUNEL method (scale bar: 100 μm). N = 5, TUNEL, terminal deoxynucleotidyl transferase dUTP nick-end labeling. ***$p < 0.001$.

increased compared with that of cells in the Control group ($p < 0.001$). This increase was reversed with the further administration of 40-μM Rg3 ($p < 0.001$).

Rg3 Inhibited CSE-induced Mitophagy and Apoptosis in BEAS-2B Cells through Upregulating SIRT1

The *SIRT1* mRNA levels shown in Fig. 3 demonstrated that SIRT1 expression in CSE-treated CEAS-2B cells was upregulated by OE-SIRT1 transfection ($p < 0.001$) and the SIRT1 expression in CSE-treated CEAS-2B cells was downregulated by sh-SIRT1 transfection ($p < 0.001$), verifying the transfection efficiency. Moreover, as shown in Fig. 4a, the SIRT1 protein level was significantly higher in CSE-treated BEAS-2B cells with OE-SIRT1 transfection and Rg3 (40 μM) administration compared with that in CSE-treated BEAS-2B cells with OE-NC transfection and Rg3 (40 μM) ($p < 0.001$). In contrast, the SIRT1 protein level was significantly lower in CSE-treated BEAS-2B cells with sh-SIRT1 transfection and Rg3 (40 μM) administration compared with that in CSE-treated BEAS-2B cells with sh-NC transfection and Rg3 (40 μM) ($p < 0.001$). Results in Fig. 4a combined with results in Fig. 4b demonstrated that the increased SIRT1 protein level in the CSE+OE-SIRT1+Medium group corresponded to decreased levels of LC3 II/I ($p < 0.001$) and PINK1 protein ($p < 0.001$). On the other hand, the decreased SIRT1 protein level in the CSE+sh-SIRT1+Medium group corresponded to increased levels of LC3 II/I ($p < 0.001$) and PINK1 protein ($p < 0.001$). We have demonstrated

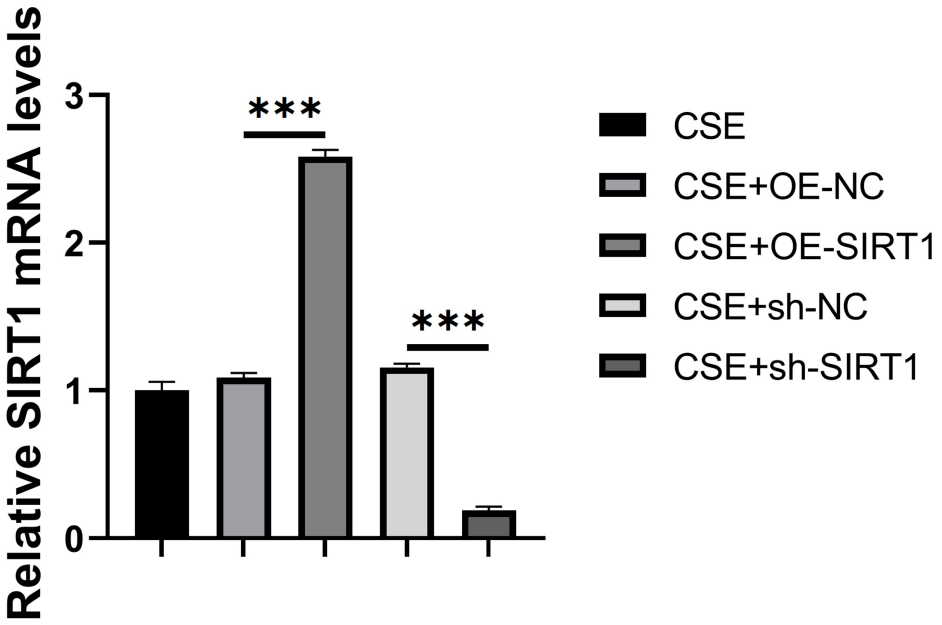

Fig. 3. SIRT1 transfection efficiency was verified. *SIRT1* mRNA levels in transfected BEAS-2B cells. N = 5. CSE+OE-NC, CSE-treated BEAS-2B cells transfected with lentiviruses containing blank vector; CSE+OE-SIRT1, CSE-treated BEAS-2B cells transfected with lentiviral vector encoding SIRT1 overexpression plasmid; CSE+sh-NC, CSE-treated BEAS-2B cells transfected with lentiviral vector encoding negative control short hairpin (sh)RNA; CSE+sh-SIRT1, CSE-treated BEAS-2B cells transfected with lentiviral vector encoding shRNA against SIRT1. ***$p < 0.001$.

that Rg3 can increase the SIRT1 level and decrease levels of LC3 II/I and PINK1 protein in CSE-treated BEAS-2B cells (Fig. 1); moreover, a further increase in SIRT1 level causes further decrease in the levels of LC3 II/I and PINK1 protein (thus inhibiting mitophagy), whereas a decrease in the SIRT1 level reversely increases the levels of LC3 II/I and PINK1 protein (thus promoting mitophagy). Together, these results demonstrate that the effect of Rg3 on inhibiting CSE-induced mitophagy in BEAS-2B cells is achieved through upregulating the SIRT1 level. Similarly, for apoptosis, we have demonstrated that the increase in the SIRT1 level induced by Rg3 was accompanied by a decrease in apoptosis in CSE-treated BEAS-2B cells (Fig. 2); Moreover, the further increase in the SIRT1 level of the CSE+OE-SIRT1+Medium group caused further decrease in apoptosis in CSE-treated BEAS-2B cells (Fig. 5; $p < 0.001$), whereas the decrease in SIRT1 level of the CSE+sh-SIRT1+Medium group reversely increased the apoptosis in CSE-treated BEAS-2B cells (Fig. 5; $p < 0.001$). Together, these results demonstrate that the effect of Rg3 on decreasing CSE-induced apoptosis in BEAS-2B cells is mediated by upregulation of the SIRT1 level.

Rg3 Improved Lung Function in CS-induced COPD Mice Models by Upregulating Sirt1 Expression

As shown in Fig. 6a,b, the levels of Sirt1 mRNA ($p < 0.001$) and Sirt1 protein ($p < 0.001$) were decreased in the Model group in which chronic CS-induced COPD murine models were established, compared with the NC group in which mice were normally cultured. The decrease in Sirt1 level was reversely upregulated by Rg3 administration (mRNA, $p < 0.001$; protein, $p < 0.001$). Moreover, for Rg3-treated COPD model mice, the infection of OE-Sirt1 increased the level of Sirt1 compared with the infection of OE-nc (mRNA, $p < 0.001$; protein, $p < 0.001$) and the infection of sh-Sirt1 decreased the level of Sirt1 compared with the infection of sh-nc (mRNA, $p < 0.001$; protein, $p < 0.001$). We found that compared with mice in the NC group, mice in the Model group had higher levels of functional residual capacity (FRC; Fig. 6c, $p < 0.001$) and lower levels of forced expiratory volume in 100 ms (FEV0.1)/forced vital capacity (FEVC) (Fig. 6d, $p < 0.001$). Mice in the Model group had higher levels of airway resistance (AR; Fig. 6e, $p < 0.001$) and lower levels of dynamic compliance (Fig. 6f; $p < 0.001$), all of which indicate impaired lung function all of which were reversed by Rg3 administration (FRC, $p < 0.01$; AR, $p < 0.01$; FEV0.1/FVC, $p < 0.05$; dynamic compliance, $p < 0.001$). These results demonstrate that Rg3 can improve lung function impaired by CS-induced COPD. Compared to Rg3-treated COPD mice models, the further upregulation of Sirt1 in Model+Rg3+OE-Sirt1 led to a further decrease in FRC ($p < 0.01$) and AR ($p < 0.05$) as well as a further increase in FEV0.1/FVC ($p < 0.05$) and dynamic compliance ($p < 0.05$), whereas downregulation of Sirt1 in Model+Rg3+sh-Sirt1 reversely increased FRC ($p < 0.01$) and AR ($p < 0.01$) as well as reversely de-

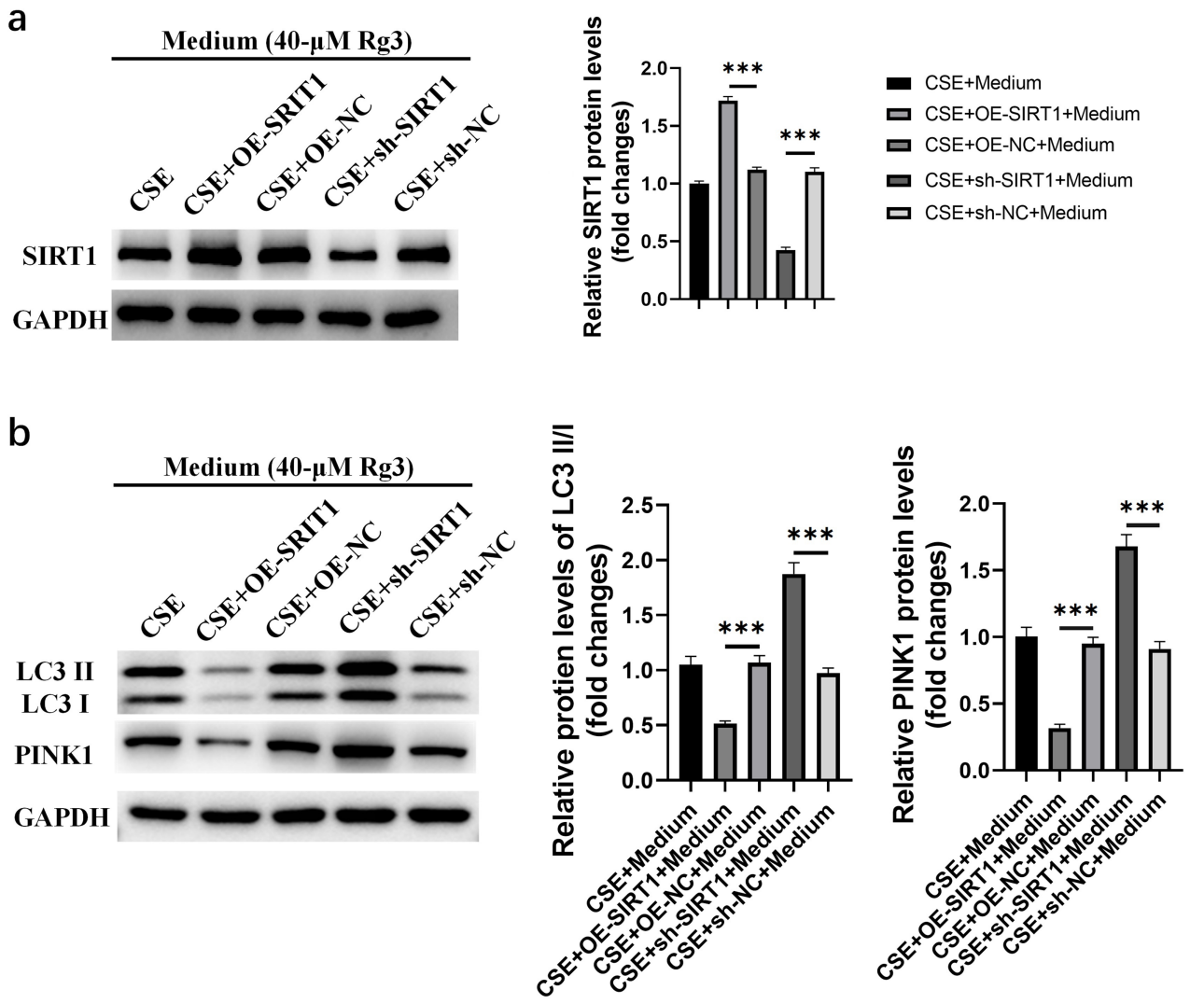

Fig. 4. Rg3 inhibited CSE-induced mitophagy in BEAS-2B cells by upregulating SIRT1. (a) The expression levels of SIRT1 protein. (b) Detection of mitophagy-related proteins. N = 5. CSE+OE-NC+Medium, CSE-treated BEAS-2B cells transfected with lentiviruses containing blank vector and administered 40-μM Rg3; CSE+OE-SIRT1+Medium, CSE-treated BEAS-2B cells transfected with lentiviruses containing SIRT1 overexpression plasmid and administered 40-μM Rg3; CSE+sh-NC+Medium, CSE-treated BEAS-2B cells transfected with lentiviruses containing vector inserted with negative control short hairpin (sh)RNA and administered 40-μM Rg3; CSE+sh-SIRT1+Medium, CSE-treated BEAS-2B cells transfected with lentiviruses containing vector inserted with shRNA of SIRT1 and administered 40-μM Rg3. ***$p < 0.001$.

creased FEV0.1/FVC ($p < 0.05$) and dynamic compliance ($p < 0.05$). Together, these results demonstrate that Rg3 improved the lung function in COPD mice models by upregulating Sirt1 levels.

Rg3 Reduced Lung Tissue Inflammation in CS-induced COPD Mice Models by Upregulating Sirt1 Expression

As shown, the levels of IL-6 (Fig. 6g, $p < 0.001$) and KC (Fig. 6h, $p < 0.001$) were increased in the Model group compared with the NC group, indicating increased inflammation in lung tissues. Administration of Rg3 in mice models decreased levels of both IL-6 (Fig. 6g, $p < 0.001$) and KC (Fig. 6h, $p < 0.001$), indicating the effect of Rg3 on reducing inflammation of lung tissues in COPD mice models. Moreover, compared to Rg3-treated mice models, the further upregulation of Sirt1 in Model+Rg3+OE-Sirt1 led to a further decrease in IL-6 (Fig. 6g, $p < 0.05$) and KC (Fig. 6h, $p < 0.01$), whereas downregulation of Sirt1 in Model+Rg3+sh-Sirt1 reversely increased IL-6 (Fig. 6g, $p < 0.01$) and KC levels (Fig. 6h, $p < 0.01$). Thus, Rg3 reduced the lung inflammation in COPD mice models by upregulating Sirt1 levels.

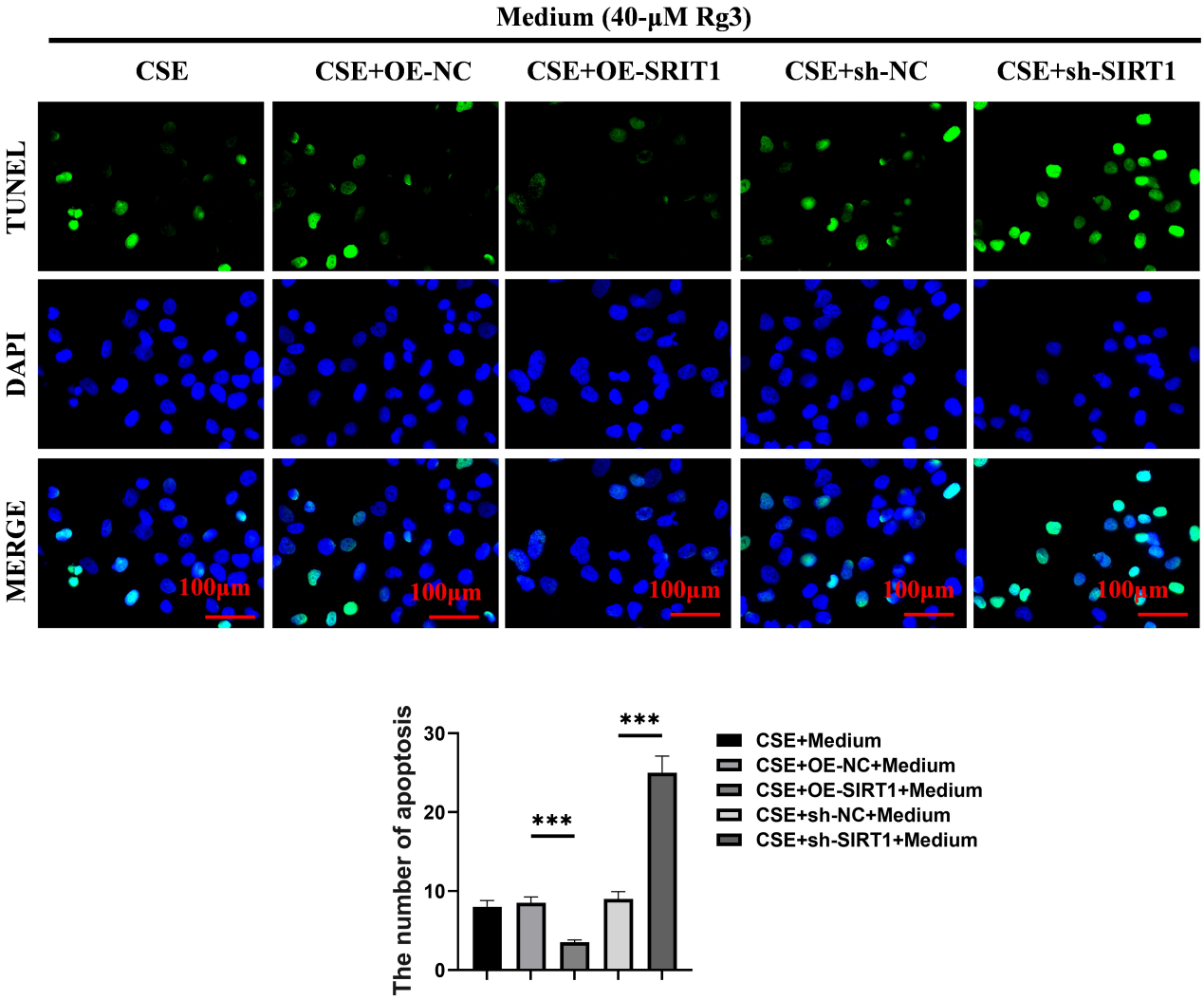

Fig. 5. Rg3 inhibited CSE-induced apoptosis in BEAS-2B cells by upregulating SIRT1. Apoptosis was detected by the TUNEL method (scale bar: 100 μm). N = 5. ***$p < 0.001$.

Rg3 Reduced Lung Impairment in CS-induced COPD Mice Models by Upregulating Sirt1 Expression

As shown in Fig. 7 the MLI in lung tissues obtained from the Model group was increased compared with that in lung tissues obtained from the NC group ($p < 0.001$), indicating a severe morphological impairment in the lungs of COPD mice. Rg3 administration decreased the MLI ($p < 0.001$) in the Model+Rg3 group, demonstrating that Rg3 reduced the impairment of lung tissues induced by COPD. Furthermore, compared to Rg3-treated mice models, the further upregulation of Sirt1 in the Model+Rg3+OE-Sirt1 group further decreased the MLI ($p < 0.01$), whereas downregulation of Sirt1 in the Model+Rg3+sh-Sirt1 group reversely increased the MLI ($p < 0.05$). Thus, Rg3 reduced the lung impairment in COPD mice models by upregulating Sirt1 levels. These findings can be directly observed in the representative images of H&E stained lung tissues, showing the bronchial epithelial tissue destruction and enlarged airspaces expansion with thicker alveolar septum in the Model group compared to the NC group, which were ameliorated by Rg3 treatment. Compared with lung tissues of Rg3-treated COPD mice, the upregulation of Sirt1 further ameliorated the morphological impairment, whereas the downregulation of Sirt1 exacerbated the impairment.

Discussion

COPD, encompassing emphysema and chronic bronchitis [32], causes impaired respiratory function for the 16 million Americans diagnosed with the condition [33]. With the global spread of the novel coronavirus epidemic, COPD patients are also more likely to be infected with COVID-19, leading to aggravation of their COPD symptoms [34–36]. Therefore, we urgently need to find a new target for the treatment of COPD.

In recent years, the application of Rg3 in lung diseases has attracted more and more attention. The previous study

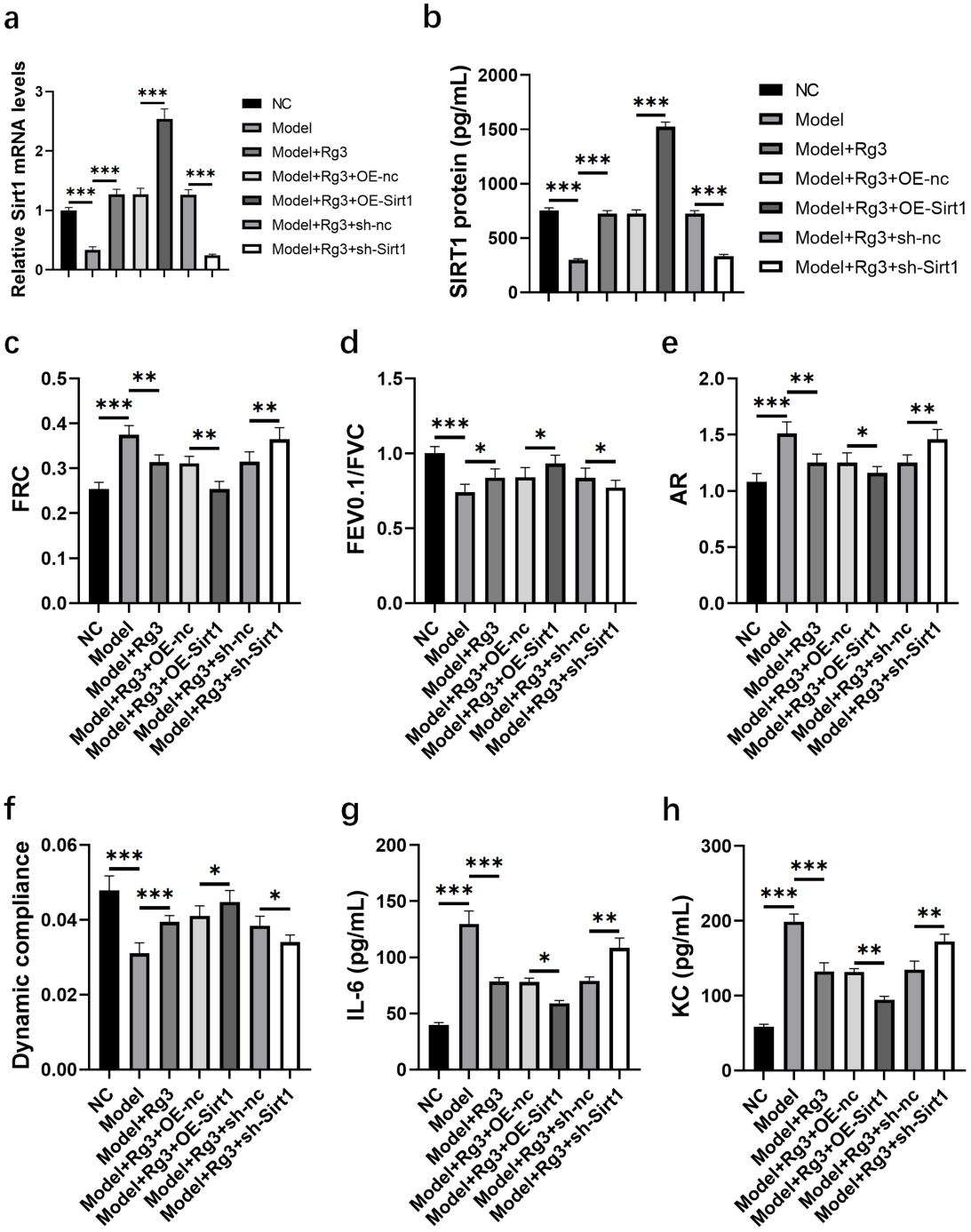

Fig. 6. Rg3 improved lung function and reduced lung inflammation in CS-induced COPD mice models by upregulating Sirt1 expression. (a) Relative mRNA levels of SIRT1 in mice models. (b) SIRT1 protein levels in mice models. (c) Levels of functional residual capacity (FRC) in mice models. (d) Levels of forced expiratory volume in 100 ms (FEV0.1)/forced vital capacity (FEVC) in mice models. (e) Levels of airway resistance (AR) in mice models. (f) Levels of dynamic compliance in mice models. (g) Levels of interleukin 6 (IL-6) in bronchial alveolar lavage fluid (BALF) from different mice models. (h) Levels of keratinocyte-derived cytokine (KC) in BALF from different mice models. N = 5. NC, negative control group of mice which were cultured normally; Model, chronic obstructive pulmonary disease (COPD) mice established by chronic CS exposure; Model+Rg3, COPD mice treated with Rg3; Model+Rg3+OE-nc, Rg3-treated COPD mice infected with lentiviruses containing blank vector; Model+Rg3+OE-Sirt1, Rg3-treated COPD mice infected with lentiviruses containing Sirt1 overexpression plasmid; Model+Rg3+sh-NC, Rg3-treated COPD mice infected with lentiviruses containing vector inserted with negative control shRNA; Model+Rg3+sh-Sirt1, Rg3-treated COPD mice infected with lentiviruses containing vector inserted with shRNA of Sirt1. *$p < 0.05$, **$p < 0.01$, ***$p < 0.001$.

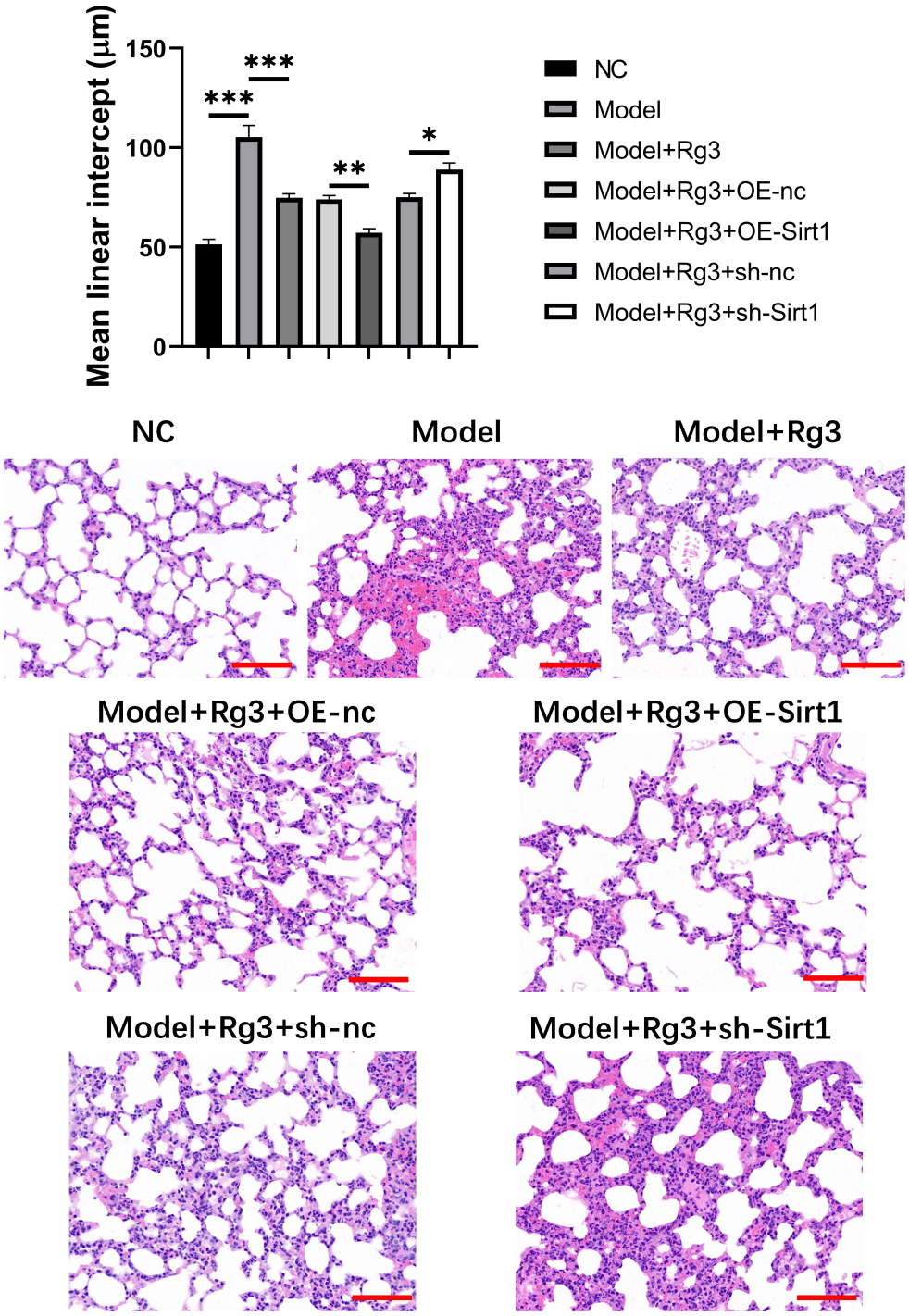

Fig. 7. Rg3 reduced lung impairment in CS-induced COPD mice models by upregulating Sirt1 expression. The levels of mean linear intercept (MLI) in lung tissues from mice models and representative images of Hematoxylin and Eosin (H&E) stained lung tissues (scale bar: 50 μm). N = 5. *$p < 0.05$, **$p < 0.01$, ***$p < 0.001$.

has shown that Rg3 can inhibit EMT that occurs during airway remodeling [37]. Therefore, we further explored the possible mechanism of Rg3 in relieving COPD through *in vivo* and *in vitro* experiments. Mitochondrial dysfunction is a key event in the pathogenesis of COPD [38]. CS exposure can cause mitochondrial damage, which is accompanied by mitophagy [39]. The previous study has also found that there is abnormal apoptosis in the bronchial epithelium of COPD rats [40]. SIRT1 is known to be closely related to mitochondrial function and apoptosis. The present study highlights the previously established anti-inflammatory and anti-tumor properties of Rg3. By demonstrating its abil-

ity to reverse the effects of CSE on SIRT1 expression and mitigate the associated cellular changes, this study supports Rg3 as a potential therapeutic agent for COPD. The findings suggest a role for Rg3 in regulating mitophagy and apoptosis in human BEAS-2B cells exposed to CSE. The upregulation of SIRT1 by Rg3 is associated with a decrease in mitophagy markers (LC3 II/I, PINK1) and cell apoptosis, indicating a potential mechanism for Rg3's protective effects. *In vivo* experiments using CS-induced COPD mice models demonstrate that Rg3 can reverse COPD-induced decreases in SIRT1 expression and lung function, and can reverse increases in pro-inflammatory markers (IL-6, KC), lung impairment, and mean linear intercept (MLI). This suggests a potential therapeutic role for Rg3 in ameliorating COPD-related lung damage. This study emphasizes the pivotal role of SIRT1 in mediating the protective effects of Rg3. Modulating SIRT1 levels affects mitophagy, apoptosis, and the overall response to COPD-related insults. These results shed light on the intricate molecular mechanisms underlying Rg3's therapeutic actions.

In conclusion, this study suggests that Rg3 may have therapeutic potential in mitigating COPD-related cellular changes, inflammation, and lung damage. The involvement of SIRT1, mitophagy, and apoptosis in these effects warrants further exploration. While the findings provide a foundation for future research and potential clinical applications, additional studies are needed to address the limitations and facilitate the translation of Rg3 into a viable COPD treatment option.

Conclusion

Our study demonstrated that Rg3 inhibits mitophagy and apoptosis of CSE-treated bronchial epithelial cells, and ameliorates COPD in mice models by upregulating SIRT1 expression. This study demonstrates that Rg3 could be potentially used as a novel medication for treating COPD.

Availability of Data and Materials

Data to support the findings of this study are available on reasonable request from the corresponding author.

Author Contributions

YYW, NZZ and HH performed the research. GT, NZZ and FL provided help and advice on the experiments. JZ, FL and GT contributed to the analysis and interpretation of the data. All authors were involved in the drafting and critical revision of the manuscript. All authors read and approved the final manuscript. All authors have participated sufficiently in the work to take public responsibility for appropriate portions of the content and agreed to be accountable for all aspects of the work in ensuring that questions related to its accuracy or integrity.

Ethics Approval and Consent to Participate

This study has been approved by the ethics committee of Anhui University of Chinese Medicine (approval no. AHUCM-rats-2021064).

Acknowledgment

Not applicable.

Funding

This research was funded by National Natural Science Foundation of China, 82174312; Anhui Provincial Administration of Traditional Chinese Medicine, Collaborative Research Project of Traditional Chinese and Western Medicine for Major and Difficult Diseases (COPD) in Anhui Province, 2021zdynjb02; Anhui Province Administration of Traditional Chinese Medicine, Anhui Province Traditional Chinese Medicine Inheritance and Innovation Research Project in 2024, 2024CCCX028.

Conflict of Interest

The authors declare no conflict of interest.

References

[1] Vogelmeier CF, Román-Rodríguez M, Singh D, Han MK, Rodríguez-Roisin R, Ferguson GT. Goals of COPD treatment: Focus on symptoms and exacerbations. Respiratory Medicine. 2020; 166: 105938.

[2] Vij N, Chandramani-Shivalingappa P, Van Westphal C, Hole R, Bodas M. Cigarette smoke-induced autophagy impairment accelerates lung aging, COPD-emphysema exacerbations and pathogenesis. American Journal of Physiology. Cell Physiology. 2018; 314: C73–C87.

[3] Albertson TE, Chenoweth JA, Pearson SJ, Murin S. The pharmacological management of asthma-chronic obstructive pulmonary disease overlap syndrome (ACOS). Expert Opinion on Pharmacotherapy. 2020; 21: 213–231.

[4] Criner GJ, Celli BR, Brightling CE, Agusti A, Papi A, Singh D, *et al*. Benralizumab for the Prevention of COPD Exacerbations. The New England Journal of Medicine. 2019; 381: 1023–1034.

[5] Hwang SK, Jeong YJ, Cho HJ, Park YY, Song KH, Chang YC. Rg3-enriched red ginseng extract promotes lung cancer cell apoptosis and mitophagy by ROS production. Journal of Ginseng Research. 2022; 46: 138–146.

[6] Wang J, Zeng L, Zhang Y, Qi W, Wang Z, Tian L, *et al*. Pharmacological properties, molecular mechanisms and therapeutic potential of ginsenoside Rg3 as an antioxidant and anti-inflammatory agent. Frontiers in Pharmacology. 2022; 13: 975784.

[7] Guan X, Yuan Y, Wang G, Zheng R, Zhang J, Dong B, *et al*. Ginsenoside Rg3 ameliorates acute exacerbation of COPD by suppressing neutrophil migration. International Immunopharmacology. 2020; 83: 106449.

[8] Yang Y, Liu Y, Wang Y, Chao Y, Zhang J, Jia Y, *et al*. Regulation of SIRT1 and Its Roles in Inflammation. Frontiers in Immunology. 2022; 13: 831168.

[9] Podyacheva E, Toropova Y. The Role of NAD+, SIRTs Interac-

tions in Stimulating and Counteracting Carcinogenesis. International Journal of Molecular Sciences. 2023; 24: 7925.

[10] Hsu HT, Yang YL, Chang WH, Fang WY, Huang SH, Chou SH, *et al*. Hyperbaric Oxygen Therapy Improves Parkinson's Disease by Promoting Mitochondrial Biogenesis via the SIRT-1/PGC-1α Pathway. Biomolecules. 2022; 12: 661.

[11] Zeng C, Chen M. Progress in Nonalcoholic Fatty Liver Disease: SIRT Family Regulates Mitochondrial Biogenesis. Biomolecules. 2022; 12: 1079.

[12] Zhang XS, Lu Y, Li W, Tao T, Peng L, Wang WH, *et al*. Astaxanthin ameliorates oxidative stress and neuronal apoptosis via SIRT1/NRF2/Prx2/ASK1/p38 after traumatic brain injury in mice. British Journal of Pharmacology. 2021; 178: 1114–1132.

[13] Shan H, Li X, Ouyang C, Ke H, Yu X, Tan J, *et al*. Salidroside prevents PM2.5-induced BEAS-2B cell apoptosis via SIRT1-dependent regulation of ROS and mitochondrial function. Ecotoxicology and Environmental Safety. 2022; 231: 113170.

[14] Kim JY, Mondaca-Ruff D, Singh S, Wang Y. SIRT1 and Autophagy: Implications in Endocrine Disorders. Frontiers in Endocrinology. 2022; 13: 930919.

[15] Wang L, Xu C, Johansen T, Berger SL, Dou Z. SIRT1 - a new mammalian substrate of nuclear autophagy. Autophagy. 2021; 17: 593–595.

[16] Lee J, Kim J, Lee JH, Choi YM, Choi H, Cho HD, *et al*. SIRT1 Promotes Host Protective Immunity against *Toxoplasma gondii* by Controlling the FoxO-Autophagy Axis via the AMPK and PI3K/AKT Signalling Pathways. International Journal of Molecular Sciences. 2022; 23: 13578.

[17] Zheng Y, Kou J, Wang P, Ye T, Wang Z, Gao Z, *et al*. Berberine-induced TFEB deacetylation by SIRT1 promotes autophagy in peritoneal macrophages. Aging. 2021; 13: 7096–7119.

[18] Wen S, Xu M, Zhang W, Song R, Zou H, Gu J, *et al*. Cadmium induces mitochondrial dysfunction via SIRT1 suppression-mediated oxidative stress in neuronal cells. Environmental Toxicology. 2023; 38: 743–753.

[19] Li HR, Liu Q, Zhu CL, Sun XY, Sun CY, Yu CM, *et al*. β-Nicotinamide mononucleotide activates NAD+/SIRT1 pathway and attenuates inflammatory and oxidative responses in the hippocampus regions of septic mice. Redox Biology. 2023; 63: 102745.

[20] Zhang Y, Li T, Pan M, Wang W, Huang W, Yuan Y, *et al*. SIRT1 prevents cigarette smoking-induced lung fibroblasts activation by regulating mitochondrial oxidative stress and lipid metabolism. Journal of Translational Medicine. 2022; 20: 222.

[21] Wu H, Ma H, Wang L, Zhang H, Lu L, Xiao T, *et al*. Regulation of lung epithelial cell senescence in smoking-induced COPD/emphysema by microR-125a-5p via Sp1 mediation of SIRT1/HIF-1a. International Journal of Biological Sciences. 2022; 18: 661–674.

[22] Kato R, Mizuno S, Kadowaki M, Shiozaki K, Akai M, Nakagawa K, *et al*. Sirt1 expression is associated with CD31 expression in blood cells from patients with chronic obstructive pulmonary disease. Respiratory Research. 2016; 17: 139.

[23] Guan R, Wang J, Cai Z, Li Z, Wang L, Li Y, *et al*. Hydrogen sulfide attenuates cigarette smoke-induced airway remodeling by upregulating SIRT1 signaling pathway. Redox Biology. 2020; 28: 101356.

[24] Tu C, Wan B, Zeng Y. Ginsenoside Rg3 alleviates inflammation in a rat model of myocardial infarction via the SIRT1/NF-κB pathway. Experimental and Therapeutic Medicine. 2020; 20: 238.

[25] Ma CH, Chou WC, Wu CH, Jou IM, Tu YK, Hsieh PL, *et al*. Ginsenoside Rg3 Attenuates TNF-α-Induced Damage in Chondrocytes through Regulating SIRT1-Mediated Anti-Apoptotic and Anti-Inflammatory Mechanisms. Antioxidants (Basel, Switzerland). 2021; 10: 1972.

[26] Kaarniranta K, Blasiak J, Liton P, Boulton M, Klionsky DJ, Sinha D. Autophagy in age-related macular degeneration. Autophagy. 2023; 19: 388–400.

[27] Zhou WC, Qu J, Xie SY, Sun Y, Yao HW. Mitochondrial Dysfunction in Chronic Respiratory Diseases: Implications for the Pathogenesis and Potential Therapeutics. Oxidative Medicine and Cellular Longevity. 2021; 2021: 5188306.

[28] Song Q, Chen P, Liu XM. The role of cigarette smoke-induced pulmonary vascular endothelial cell apoptosis in COPD. Respiratory Research. 2021; 22: 39.

[29] Sun X, Feng X, Zheng D, Li A, Li C, Li S, *et al*. Ergosterol attenuates cigarette smoke extract-induced COPD by modulating inflammation, oxidative stress and apoptosis *in vitro* and *in vivo*. Clinical Science (London, England: 1979). 2019; 133: 1523–1536.

[30] Long C, Lai Y, Li T, Nyunoya T, Zou C. Cigarette smoke extract modulates *Pseudomonas aeruginosa* bacterial load via USP25/HDAC11 axis in lung epithelial cells. American Journal of Physiology. Lung Cellular and Molecular Physiology. 2020; 318: L252–L263.

[31] Dunnill MS. EVALUATION OF A SIMPLE METHOD OF SAMPLING THE LUNG FOR QUANTITATIVE HISTOLOGICAL ANALYSIS. Thorax. 1964; 19: 443–448.

[32] Kim V, Criner GJ. Chronic bronchitis and chronic obstructive pulmonary disease. American Journal of Respiratory and Critical Care Medicine. 2013; 187: 228–237.

[33] O'Dell A, Diegel-Vacek L, Burt L, Corbridge S. CE: Managing Stable COPD: An Evidence-Based Approach. The American Journal of Nursing. 2018; 118: 36–47.

[34] Leung JM, Niikura M, Yang CWT, Sin DD. COVID-19 and COPD. The European Respiratory Journal. 2020; 56: 2002108.

[35] Christenson SA, Smith BM, Bafadhel M, Putcha N. Chronic obstructive pulmonary disease. Lancet (London, England). 2022; 399: 2227–2242.

[36] Wu F, Burt J, Chowdhury T, Fitzpatrick R, Martin G, van der Scheer JW, *et al*. Specialty COPD care during COVID-19: patient and clinician perspectives on remote delivery. BMJ Open Respiratory Research. 2021; 8: e000817.

[37] Mao X, Jin Y, Feng T, Wang H, Liu D, Zhou Z, *et al*. Ginsenoside Rg3 Inhibits the Growth of Osteosarcoma and Attenuates Metastasis through the Wnt/β-Catenin and EMT Signaling Pathway. Evidence-based Complementary and Alternative Medicine: ECAM. 2020; 2020: 6065124.

[38] Maremanda KP, Sundar IK, Rahman I. Role of inner mitochondrial protein OPA1 in mitochondrial dysfunction by tobacco smoking and in the pathogenesis of COPD. Redox Biology. 2021; 45: 102055.

[39] Araya J, Tsubouchi K, Sato N, Ito S, Minagawa S, Hara H, *et al*. PRKN-regulated mitophagy and cellular senescence during COPD pathogenesis. Autophagy. 2019; 15: 510–526.

[40] Wu H, Miao Y, Shang LQ, Chen RL, Yang SM. MiR-31 aggravates inflammation and apoptosis in COPD rats via activating the NF-κB signaling pathway. European Review for Medical and Pharmacological Sciences. 2020; 24: 9626–9632.